

An intersectional framework for counterfactual fairness in risk prediction

Solvejg Wastvedt* Jared Huling* Julian Wolfson*

October 5, 2022

Abstract

Along with the increasing availability of data in many sectors has come the rise of data-driven models to inform decision-making and policy. These models have the potential to benefit both patients and health care providers but can also entrench or exacerbate health inequities. Existing “algorithmic fairness” methods for measuring and correcting model bias fall short of what is needed for clinical applications in two key ways. First, methods typically focus on a single grouping along which discrimination may occur rather than considering multiple, intersecting groups such as gender and race. Second, in clinical applications, risk prediction is typically used to guide treatment, and use of a treatment presents distinct statistical issues that invalidate most existing fairness measurement techniques. We present novel unfairness metrics that address both of these challenges. We also develop a complete framework of estimation and inference tools for our metrics, including the *unfairness value* (“*u-value*”), used to determine the relative extremity of an unfairness measurement, and standard errors and confidence intervals employing an alternative to the standard bootstrap. Our framework provides new tools for health systems seeking improve equity in their use of data and risk prediction to drive policy.

*Division of Biostatistics, University of Minnesota

1 Introduction

Along with the increasing availability of data in many sectors has come the rise of data-driven models to inform decision-making by predicting outcomes like disease, hospital readmission, and many more. In health care, such *risk prediction models* are used to assess patients’ likelihood of certain adverse outcomes and guide assignment of treatments or interventions. These models have the potential to benefit both patients and health care providers by personalizing treatment and improving efficiency [24] [5].

However, risk prediction models also have the potential to entrench or exacerbate health inequities. High-profile examples of inequities perpetrated by the models, which often use opaque, “black box” machine learning techniques, have emerged both in health care contexts and elsewhere [28, 34, 4]. In response, techniques for measuring and correcting model bias, which broadly constitute the field of “algorithmic fairness”, have proliferated. These techniques include an array of definitions of model unfairness [9], most of which compare some measure of performance of the model across groups defined by a social characteristic like race or gender or an attribute such as age, income, etc.

For clinical applications, existing algorithmic fairness work falls short in two key ways. First, definitions typically focus on a single grouping along which discrimination may occur, for example assessing performance for men vs. women. This simplification fails to recognize that discrimination occurs based on many different groupings which interact in complex ways. Second, in clinical applications, risk prediction is typically used to guide treatment, and use of a treatment presents distinct statistical issues that invalidate most existing fairness measurement techniques. To our knowledge, no existing fairness work addresses both challenges; in this paper we present three novel unfairness metrics that are valid when the risk score is used to guide treatment and account for intersecting forms of

discrimination. We also develop a complete framework for estimation and inference on our metrics. For estimation, we present new procedures that restrict the error rate estimates underlying our metrics within the natural $[0, 1]$ bounds. We then present tools for inference on the summary metrics, including the *unfairness value* (“*u-value*”), used to determine the relative extremity of an unfairness measurement, and standard errors and confidence intervals. Our standard error procedure employs an alternative to the standard bootstrap necessitated by the fact that our metrics are aggregations of absolute values.

1.1 Intersectionality in health care and risk prediction

Our work falls in the emerging area of techniques addressing multiple, intersecting forms of discrimination which is typically referred to as *intersectional fairness* work. The term *intersectionality* was coined by legal scholar Kimberlé Crenshaw, although its ideas have a long history in Black feminist thought and elsewhere [33] [21]. Crenshaw used intersectionality to describe the experiences of oppression Black women face, arguing that this oppression is not simply additive, or the sum of racism and sexism, but a distinct form of discrimination that demands new analysis [13, 14]. Definitions of what exactly constitutes intersectionality are often debated, but it has been broadly characterized as a “knowledge project” engaged in by scholars and social justice activists from a wide array of disciplines whose focus is on “power relations and social inequalities” [20]. Intersectional analysis seeks to identify and dismantle interlocking forms of discrimination wherever they occur, whether based on race, sex, gender identity, class, or otherwise [22].

In health care, the importance of an intersectional approach has been firmly established by work documenting the health impacts of interlocking forms of discrimination. As a recent example, the COVID-19 pandemic has disproportionately hurt groups at the intersections

of racial, gender and economic oppression in many ways, including disproportionate health consequences for Black Americans [1] and job losses unequally borne by Latina women [2]. Clinical risk models are susceptible to all these interlocking inequities. For example, researchers at a major health system decided against implementing a patient “no-show” prediction tool after realizing that it could discriminate both explicitly and implicitly based on a wide range of patient characteristics [32].

1.2 The need for counterfactual fairness

In clinical settings, risk prediction typically informs and is accompanied by assignment of some treatment, for example care coordination services or intensive COVID-19 therapies. In this setting, we wish to predict the risk to a patient were they to remain untreated and thereby target our intervention to those at highest risk. However, when a treatment is in use, data available for fairness assessment consists of a mix of outcomes observed with treatment and without. Moreover, if the treatment is more often applied or is more effective in certain groups, the mismatch between desired prediction targets and available data is more severe for these groups. Conventional methods for assessing performance will fail in this situation, especially for groups where the mismatch is greatest. Fairness measurements that fail to account for this phenomenon will also fail and could falsely ascribe fairness to a model that in fact discriminates against one group.

1.2.1 Using potential outcomes to measure performance

This failure is the motivation for a recent, non-intersectional approach to algorithmic fairness called *counterfactual fairness* which uses techniques from causal inference [12] [29]. These metrics replace observed outcomes with *potential outcomes*, or the outcomes that

would have been observed under a given treatment decision. Using potential outcomes allows us to assess a model’s performance and fairness relative to a baseline in which no patients are treated, thus avoiding the bias described above. The counterfactual quantities are estimated from observed data and used in a common model fairness criterion.

1.2.2 Related work

This counterfactual framework differs from a similarly named area of work in which counterfactuals are with respect to the protected characteristic rather than treatment assignment [39] [26]. This alternative framework considers potential outcomes in a world in which a person belonged to a different group, e.g. were of a different race or gender. However, the validity of causal assumptions in this approach is difficult to establish, particularly in the case of socially constructed characteristics like race or gender [15, 35]. Further, this is not the relevant counterfactual for settings in which risk predictors guide interventions [12], so we do not take this approach

Elsewhere, existing work has proposed measurements for fairness across multiple intersecting characteristics [31, 16] and methods for training fairer models (e.g. [19, 23, 38, 41]), but these methods do not account for the bias due to treatment described in this section.

2 Existing definitions and statistical framework

In this section, we describe a statistical framework for measuring counterfactual equalized odds with a single protected characteristic [29] and our extension of this framework to the intersectional context.

Following convention in algorithmic fairness work, define a *protected characteristic* as any grouping, such as race or gender, along which we wish to measure discrimination. Let

A denote a protected characteristic, which [29] assume is binary. Let S denote a binary risk prediction; note that although many clinical risk models produce predicted probabilities, we are using the binary prediction derived by selecting a cut-off threshold. Let D denote a binary treatment assignment and Y a binary outcome such as an adverse health event. Under a binary treatment, there are two potential outcomes: Y^0 , the outcome under no treatment, and Y^1 , the outcome under treatment. The Y^0 outcome is the most relevant quantity in many clinical risk prediction settings, where we aim to predict patients' baseline risk in order to guide treatment. The following counterfactual quantities, defined in [29] and [12], substitute the Y^0 potential outcome for Y in common model performance and fairness metrics.

Definition 1. *The counterfactual false positive rate of a predictor S for protected group $A = a$, denoted $cFPR(S, a)$, is equal to $Pr(S = 1|Y^0 = 0, A = a)$. The counterfactual false negative rate, $cFNR(S, a)$, is equal to $Pr(S = 0|Y^0 = 1, A = a)$.*

These quantities are counterfactual analogues to the commonly used false positive and false negative rates, referred to as *observational error rates*.

When D , S , A , and Y^0 are binary, equality of the counterfactual false positive rate and counterfactual false negative rate between the levels of A is equivalent to a counterfactual version of the common fairness metric *equalized odds*.

Definition 2. *For $A, D, S, Y^0 \in \{0, 1\}$, a predictor S satisfies counterfactual equalized odds if $cFPR(S, 0) = cFPR(S, 1)$ and $cFNR(S, 0) = cFNR(S, 1)$.*

We take counterfactual equalized odds as the starting point for our metrics because of its relevance to clinical settings, where a typical performance metric of interest is a model's ability to correctly identify patients who need treatment (minimize counterfactual false negatives) and not erroneously recommend treatment for patients who do not need it

(minimize counterfactual false positives). A predictor satisfying counterfactual equalized odds is “fair” in the sense that its accuracy is the same across protected characteristic groups.

A key parameter controlling group-specific counterfactual error rates, and therefore counterfactual unfairness, is defined in [29] as the *intervention strength*. This parameter describes the effectiveness of the treatment for a given protected group.

Definition 3. Intervention strength: *The probability of not having the event under treatment, for protected group $A = a$, given that the event would have occurred with no treatment, $P(Y^1 = 0|D = 1, Y^0 = 1, A = a)$.*

To see the connection between the intervention strength and counterfactual error rates, consider a scenario with two simplifying assumptions: a predictor with fixed observational error rates, and the assumption that treatment never increases the chance of an adverse outcome (i.e. $P(Y^1 = 1|Y^0 = 0) = 0$). As explained in [29], the counterfactual error rate for a given group is then driven by the extent to which potential outcomes Y^0 differ from observed outcomes Y in that group. Because we have assumed $Y^1 = 0$ whenever $Y^0 = 0$, the only way Y^0 and Y can differ is when $Y^0 = 1$ and $Y = 0$, or equivalently (under our causal assumptions) when $Y^0 = 1$, $D = 1$, and $Y^1 = 0$. As noted in the definition, the probability that $Y^1 = 0$ given $Y^0 = 1$ and $D = 1$ is the intervention strength. By altering a group’s intervention strength, we therefore alter counterfactual error rates for the group. Thus different intervention strengths among protected groups can create counterfactual unfairness even when a predictor is fair on observational measures.

To quantify counterfactual fairness, [29] define the *counterfactual error rate differences* of a predictor S , denoted $\Delta^+(S)$ and $\Delta^-(S)$, as the differences in counterfactual false positive and false negative rates between two groups of the single protected characteristic

$A \in \{0, 1\}$.

$$\Delta^+(S) = cFPR(S, 0) - cFPR(S, 1) \tag{1}$$

$$\Delta^-(S) = cFNR(S, 0) - cFNR(S, 1) \tag{2}$$

3 Estimands

We now extend counterfactual error rates to the intersectional context and propose three novel summary metrics that can be used to assess the unfairness of a risk prediction model. In all estimands, we accommodate the intersectional context by replacing the single protected characteristic, A , with the vector \mathbf{A} . Let m be the number of protected characteristics that we wish to consider. Denote the characteristics A_j , $j \in \{1, \dots, m\}$ and assume each A_j is a categorical variable with a finite number of levels, the set of which is denoted \mathcal{A}_j . Let $\mathbf{A} = \{A_1, A_2, \dots, A_m\}^T \in \mathcal{A}$ contain all protected characteristics of interest, where \mathcal{A} is the set of all possible combinations of all levels of the m characteristics.

Under this notation, we denote the counterfactual error rate differences between the group having protected characteristic vector \mathbf{a} and the group having \mathbf{a}' as $\Delta^+(S, \mathbf{a}, \mathbf{a}')$ (difference in counterfactual false positive rates) and $\Delta^-(S, \mathbf{a}, \mathbf{a}')$ (difference in counterfactual false negative rates).

$$\Delta^+(S, \mathbf{a}, \mathbf{a}') = cFPR(S, \mathbf{a}) - cFPR(S, \mathbf{a}') \tag{3}$$

$$\Delta^-(S, \mathbf{a}, \mathbf{a}') = cFNR(S, \mathbf{a}) - cFNR(S, \mathbf{a}') \tag{4}$$

We use the general $\Delta(S, \mathbf{a}, \mathbf{a}')$ throughout to denote either the positive ($\Delta^+(S, \mathbf{a}, \mathbf{a}')$) or negative ($\Delta^-(S, \mathbf{a}, \mathbf{a}')$) version of the counterfactual error rate difference. The relative consequences of false positives and false negatives can vary widely by situation, so the version of the metric that is of most interest will also vary. The general notation $\Delta(S, \mathbf{a}, \mathbf{a}')$ also opens the possibility that a metric other than $cFPR$ or $cFNR$ could be compared, such as area under a counterfactual version of the receiver operating characteristic (ROC) curve, although we leave this extension to future work.

3.1 Novel summary unfairness metrics

Our first metric provides an overall picture of the unfairness among all possible combinations of the protected characteristics.

Definition 4. Average intersectional counterfactual unfairness *is the average of absolute error rate differences across all possible pairs of protected characteristic vectors.*

$$\Delta_{AVG}(S) = \frac{1}{|\mathcal{A}|} \sum_{\mathbf{a}, \mathbf{a}' \in \mathcal{A}} |\Delta(S, \mathbf{a}, \mathbf{a}')| \quad (5)$$

When one group displays extreme unfairness and differences among all other groups are small, Δ_{AVG} is pulled downwards by the smaller differences and fails to capture the full extent of the unfairness. The problem is worse if the number of intersectional groups is large, since then Δ_{AVG} has even less sensitivity to unfairness involving only one or a few groups. These facts motivate our second metric.

Definition 5. Maximum intersectional counterfactual unfairness *is the maximum absolute error rate difference across all combinations of protected characteristics.*

$$\Delta_{MAX}(S) = \max_{\mathbf{a}, \mathbf{a}' \in \mathcal{A}} |\Delta(S, \mathbf{a}, \mathbf{a}')| \quad (6)$$

In some contexts, it may be desirable to capture changes in the spread of error rate differences rather than simply their relative sizes. If error rates are equally spaced, such that there are relatively large differences among all groups, this suggests a different issue than if one extreme difference is driving the measurement. The desire to measure spread of error rate differences motivates our third metric.

Definition 6. Variational intersectional counterfactual unfairness *is the variance of absolute error rate differences across all combinations of protected characteristics.*

$$\Delta_{VAR}(S) = \frac{1}{|\mathcal{A}| - 1} \sum_{\mathbf{a}, \mathbf{a}' \in \mathcal{A}} (|\Delta(S, \mathbf{a}, \mathbf{a}')| - \Delta_{AVG})^2 \quad (7)$$

4 Comparisons of novel unfairness metrics

As noted in the previous section, no single metric can fully assess the fairness properties of a model. Here we demonstrate more fully, using a hypothetical clinical example and simulation, the ways in which multiple metrics give practitioners a fuller picture. We also compare our approach to two metrics that follow immediately from existing work and are either counterfactual or intersectional, but not both. The first of these metrics is not intersectional; it simply adds additional protected characteristics, in a non-intersecting manner, to the counterfactual error rate differences metric proposed by [29]. We refer to this metric as “marginal” and denote it Δ_{MARG} .

$$\Delta_{MARG}(S) = \frac{1}{\mathcal{A}^*} \sum_{j=1}^m \sum_{a_j, a'_j \in \mathcal{A}_j} |\Delta(S, a_j, a'_j)| \quad (8)$$

where \mathcal{A}^* is the count of pairs within protected groups, i.e. $\mathcal{A}^* = \sum_{j=1}^m \binom{|\mathcal{A}_j|}{2}$.

The second comparison metric, proposed in [31], is not counterfactual; we refer to it as “observational” and denote it Δ_{OBS} .

$$\Delta_{OBS}(S) = \frac{1}{|\mathcal{A}|} \sum_{\mathbf{a}, \mathbf{a}' \in \mathcal{A}} |\Delta_O(S, \mathbf{a}, \mathbf{a}')| \quad (9)$$

where $\Delta_O(S, \mathbf{a}, \mathbf{a}')$ is the difference in observational false positive or false negative rates between the group having protected characteristic vector \mathbf{a} and the group having \mathbf{a}' .

We now demonstrate the strengths of our novel unfairness metrics, relative to these comparisons and relative to each other, using a hypothetical scenario.

4.1 Hypothetical clinical example and simulation

Suppose a hospital is treating a surge of COVID-19 patients and has a limited supply of an effective antiviral therapy. The hospital creates a prediction model to estimate patients’ risk of severe COVID-19 at hospital admission based on factors like symptoms and pre-existing conditions. Suppose preliminary work indicated the model may have issues with fair prediction based on patient age, which we denote A_1 in our simulation, and gender, which we denote A_2 . We assume that the hospital is primarily interested in the counterfactual false negative rate of the predictor, i.e. its ability to identify patients in need of treatment. We make the simplifying assumptions that age and gender are categorized in a binary fashion, as older/younger and men/women. The treatment and outcome (severe COVID-19) are also binary. In this hypothetical example, younger patients and women are less common, making younger women the numeric minority. We assume a model with poorest performance, as measured by highest counterfactual false negative rate, for the minority group (younger women), better performance for groups with just one of age or gender set

to the smaller value, and best for the majority group (older men). Data generation details for this simulation are given in the Supplementary Material.

4.2 Need for a counterfactual metric: Δ_{AVG} versus Δ_{OBS}

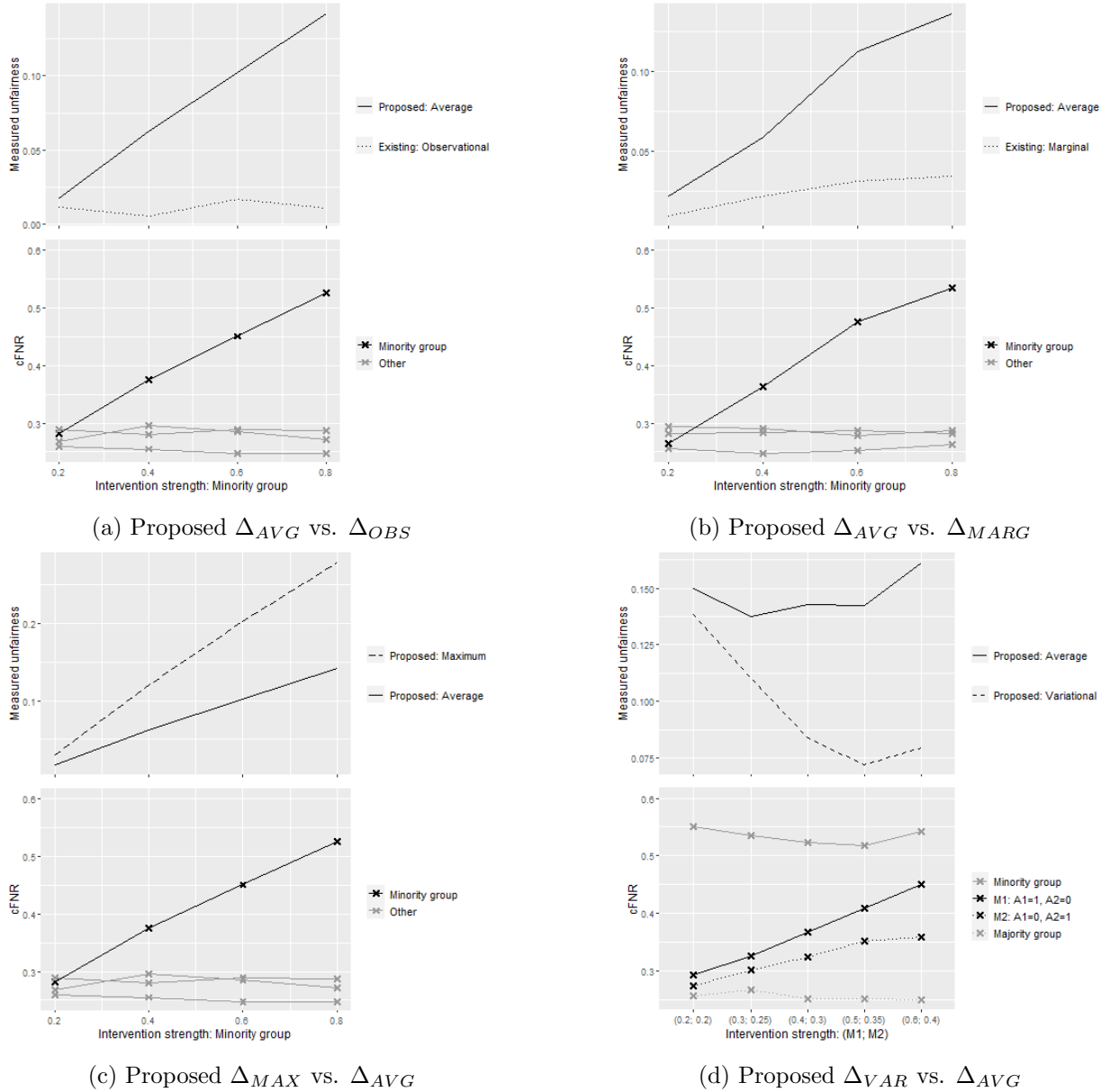


Figure 1: Top of each panel: Performance of metrics using the true error rates of the risk model as established with a validation set of size 50,000. Bottom of each panel: Group-specific true $cFNR$ values as established using the validation set.

First, we compare our intersectional, counterfactual Δ_{AVG} to the non-counterfactual

(but intersectional) Δ_{OBS} , in an extension of the example [29] use to justify their measure. Figure 1a shows scenarios with increasing counterfactual false negative rate ($cFNR$) for the minority group, moving right along the x-axis, while the $cFNR$ for the other groups does not change (Figure 1a, bottom panel). This change is driven by increasing intervention strength for the minority group compared to all others, as explained in Section 2.

In our hypothetical example, the right side of the graph corresponds to a situation in which the antiviral therapy is considerably more effective in younger women than in any other group, and the $cFNR$ is highest for this group.

As the counterfactual false negative rate increases for the minority group, Δ_{OBS} (dotted line) fails to capture any of the changing unfairness since the change is in counterfactual and not observational error rates (Figure 1a, top panel). In contrast, our Δ_{AVG} (solid line) does capture the increasing unfairness. In our clinical example, Δ_{AVG} would show the increasing disadvantage to younger women perpetrated by the model, while Δ_{OBS} would not.

4.3 Need for an intersectional metric: Δ_{AVG} versus Δ_{MARG}

To further demonstrate the need for our counterfactual, intersectional metrics, we consider a new scenario with an even smaller minority group. We then manipulate the minority group’s intervention strength as in the previous scenario. Again, the counterfactual false negative rate for the minority group increases while rates for other groups remain small. As shown in Figure 1b, Δ_{MARG} (dotted line) fails to fully capture the increasing unfairness involving this small group. In contrast, our proposed Δ_{AVG} (solid line) provides a clearer picture of the increasing unfairness and its magnitude.

To understand this effect, note that Δ_{AVG} weights unfairness from all groups equally,

regardless of their size. In contrast, Δ_{MARG} effectively down-weights unfairness in the smallest groups. In our example, the smallest group, younger women, has a small size and increasing levels of unfairness. Down-weighting this unfairness because of the group’s size, as in Δ_{MARG} , camouflages the increasingly unfair situation.

4.4 Comparison of novel metrics: Δ_{MAX} versus Δ_{AVG}

Returning to the scenario in Section 4.2, we now show how our novel metrics work together to give a full picture of unfairness. In this scenario, as the $cFNR$ increases for the minority group, disparities between this group and all other groups increase (Figure 1c, bottom panel). However, pairwise comparisons of error rates not involving the minority group do not change. As a result, Δ_{AVG} (solid line) partially hides the increasing disparities by including the smaller differences in the average, while Δ_{MAX} (dotted line) shows a fuller picture of the increasing unfairness (Figure 1c, top panel). In our hypothetical clinical example, considering Δ_{MAX} alongside Δ_{AVG} would allow the hospital to learn the full extent of the model’s inability to predict correctly for younger women.

This is not to suggest that Δ_{MAX} always provides optimal insight into unfairness. Suppose, in our example, that the hospital is comparing two potential models. If both have equal unfairness between the most disparate groups, Δ_{MAX} will grade the models identically. But suppose one model has greater unfairness between another pair, such as older men and younger men. In this case, to see the fairness difference we need a measure such as Δ_{AVG} that considers unfairness across all pairwise comparisons, making Δ_{MAX} and Δ_{AVG} complementary metrics.

4.5 Comparison of novel metrics: Δ_{VAR} versus Δ_{AVG}

Finally, we show the added insight Δ_{VAR} can provide by considering a slightly different scenario. On the left side of Figure 1d (bottom panel), the minority group has noticeably higher error rates than any other group. In this case, the high value of Δ_{VAR} relative to Δ_{AVG} signals the uneven spread of error rates and the disadvantage specific to one group. In our hypothetical example, evaluating Δ_{AVG} and Δ_{VAR} together in this scenario would encourage the hospital to focus on improving predictions for the single poorly-predicted group.

Moving from left to right in Figure 1d, however, counterfactual false negative rates increase for the two middle-sized groups, denoted “M1” (A_1 set to 1) and “M2” (A_2 set to 1). On the right side of Figure 1d (bottom panel), the error rates are more evenly spaced meaning unfairness is the result of disparities involving several pairs. While Δ_{AVG} remains approximately the same as at the left side of the figure, Δ_{VAR} changes to be comparatively lower due to the more even spread of error rates. A low value of Δ_{VAR} relative to Δ_{AVG} suggests unfairness driven by multiple groups. In our hypothetical example, such metrics would direct the hospital to focus on improving predictions for all non-majority groups.

5 Identification

Existing work [29] has shown that the counterfactual error rates of a binary predictor S can be identified for a single binary protected characteristic, A , under standard causal inference assumptions. We make these same assumptions, substituting the protected characteristic vector \mathbf{A} for the single characteristic A . Let \mathbf{X} be a vector of observed covariates. Define the propensity score function for a given protected group as $\pi = \mathbb{P}(D = 1|A, \mathbf{X}, S)$. Then the assumptions for identification of $cFPR(S, \mathbf{a})$ and $cFNR(S, \mathbf{a})$ are:

- A1. (Consistency) The observed outcome for each subject is equal to that subject's potential outcome under the treatment actually received; i.e. $Y = DY^1 + (1 - D)Y^0$.
- A2. (Positivity) $\exists \delta \in (0, 1)$ such that $\mathbb{P}(1 - \pi(\mathbf{A}, \mathbf{X}, S) \geq \delta) = 1$.
- A3. (Ignorability) D is independent of Y^0 conditional on $\mathbf{A}, \mathbf{X}, S$.

However, we note that the doubly robust estimator [29] propose for the positive counterfactual error rate can exceed the bounds $[0, 1]$, which are natural constraints that the estimate of an error rate would ideally respect. Thus rather than using existing estimators, we derive new weighted estimators that are constrained within $[0, 1]$ for both the positive and negative counterfactual error rates. Proposition 1 shows our general result for identification of quantities with functions of the predictor S and counterfactual outcome Y^0 . A proof of Proposition 1 is provided in the Supplementary Material.

Proposition 1. *Given arbitrary bounded functions $f(S)$ and $g(Y^0)$, the following holds:*

$$E[f(S)g(Y^0)I(\mathbf{A} = \mathbf{a})] = E \left[\frac{(1 - D)f(S)g(Y)I(\mathbf{A} = \mathbf{a})}{1 - \pi(\mathbf{A}, \mathbf{X}, S)} \right]$$

We now apply Proposition 1 to identification of the counterfactual error rates of the predictor S for the group having protected characteristic vector $\mathbf{A} = \mathbf{a}$.

$$cFPR(S, \mathbf{a}) = \frac{E \left[\frac{(1-D)S(1-Y)I(\mathbf{A}=\mathbf{a})}{1-\pi(\mathbf{A}, \mathbf{X}, S)} \right]}{E \left[\frac{(1-D)(1-Y)I(\mathbf{A}=\mathbf{a})}{1-\pi(\mathbf{A}, \mathbf{X}, S)} \right]} \quad (10)$$

$$cFNR(S, \mathbf{a}) = \frac{E \left[\frac{(1-D)(1-S)YI(\mathbf{A}=\mathbf{a})}{1-\pi(\mathbf{A}, \mathbf{X}, S)} \right]}{E \left[\frac{(1-D)YI(\mathbf{A}=\mathbf{a})}{1-\pi(\mathbf{A}, \mathbf{X}, S)} \right]} \quad (11)$$

The error rate differences, $\Delta(S, \mathbf{a}, \mathbf{a}')$, are then identified as $\Delta^+(S, \mathbf{a}, \mathbf{a}') = |cFPR(S, \mathbf{a}) -$

$cFPR(S, \mathbf{a}')|$ and $\Delta^-(S, \mathbf{a}, \mathbf{a}') = |cFNR(S, \mathbf{a}) - cFNR(S, \mathbf{a}')|$. Our proposed unfairness metrics are identified by inserting the relevant error rate differences into equations 5, 6, and 7.

6 Estimation

6.1 Estimating intersectional, counterfactual unfairness metrics

To estimate our new counterfactual, intersectional unfairness metrics, we first propose estimators of the counterfactual error rates as identified in equations 10 and 11. Following the notation in Section 2, let $\{\mathbf{A}_i, D_i, Y_i, \mathbf{X}_i, S_i\}$, $i = 1, \dots, n$ be the observed data and binary predictions from the risk model.

$$\widehat{cFPR}(S, \mathbf{a}) = \frac{\sum_{i=1}^n [(1 - D_i)S_i(1 - Y_i)I\{\mathbf{A}_i = \mathbf{a}\}/(1 - \hat{\pi}_i)]}{\sum_{i=1}^n [(1 - D_i)(1 - Y_i)I\{\mathbf{A}_i = \mathbf{a}\}/(1 - \hat{\pi}_i)]} \quad (12)$$

$$\widehat{cFNR}(S, \mathbf{a}) = \frac{\sum_{i=1}^n [(1 - D_i)(1 - S_i)Y_iI\{\mathbf{A}_i = \mathbf{a}\}/(1 - \hat{\pi}_i)]}{\sum_{i=1}^n [(1 - D_i)Y_iI\{\mathbf{A}_i = \mathbf{a}\}/(1 - \hat{\pi}_i)]} \quad (13)$$

Note that the numerators and denominators of equations 12 and 13 are each weighted averages of a combination of outcome, protected characteristic, and in the case of the numerators, predictor values. For example, the denominator of $\widehat{cFPR}(S, \mathbf{a})$ is a weighted average of $(1 - Y)I(\mathbf{A} = \mathbf{a})$, with weights equal to $\frac{1-D}{1-\pi(\mathbf{A}, \mathbf{X}, S)}$.

We make two further observations about these estimators. First, as noted in the previous section, they are constrained within the natural error rate bounds of $[0, 1]$. Second, they are equivalent to versions of the estimators with normalized weights in each of the

numerators and denominators. This is because normalization would require dividing each numerator and denominator by the sum of the weights in all n observations. These sums of the weights would cancel out, leaving equations 12 and 13.

To estimate the error rate differences, we replace $cFPR(S, \mathbf{a})$ and $cFNR(S, \mathbf{a})$ in equations 3 and 4 with their estimates. Finally, to estimate our new counterfactual, intersectional unfairness metrics, we use the estimated error rate differences in equations 5, 6, and 7.

$$\widehat{\Delta}_{AVG}(S) = \frac{1}{|\mathcal{A}|} \sum_{\mathbf{a}, \mathbf{a}' \in \mathcal{A}} \left| \widehat{\Delta}(S, \mathbf{a}, \mathbf{a}') \right| \quad (14)$$

$$\widehat{\Delta}_{MAX}(S) = \max_{\mathbf{a}, \mathbf{a}' \in \mathcal{A}} \left| \widehat{\Delta}(S, \mathbf{a}, \mathbf{a}') \right| \quad (15)$$

$$\widehat{\Delta}_{VAR}(S) = \frac{1}{|\mathcal{A}| - 1} \sum_{\mathbf{a}, \mathbf{a}' \in \mathcal{A}} \left(\left| \widehat{\Delta}(S, \mathbf{a}, \mathbf{a}') \right| - \widehat{\Delta}_{AVG} \right)^2 \quad (16)$$

We estimate the non-intersectional metric Δ_{MARG} and the non-counterfactual metric Δ_{OBS} for comparison in an analogous manner.

6.2 Estimating nuisance parameters

To use these estimators, we must also estimate the propensity score function $\pi(\mathbf{A}, \mathbf{X}, S)$. We suggest two options for this estimation: a simple generalized linear model and a more flexible ensemble approach that combines multiple machine learning-based estimates, such as the super learner [27].

Because of the simple structure of the generalized linear model, we do not assume any sample splitting or cross-fitting when fitting this model and obtaining propensity scores. For the ensemble model, we use a 10-fold version of the cross-fitting procedure suggested by

[29]. For each of the 10 folds, we fit the ensemble propensity score model on the remaining data to obtain predictions for the held-out fold, thus avoiding potential overfitting.

For comparison, we include two other methods of nuisance parameter estimation in the analyses that follow. In Section 8, we use a version of expressions 12 and 13 with the propensity score calculated using the true data generating mechanism as specified in our simulation. We also include a regression estimator, in which we replace the quantity $(1 - Y_i)(1 - D_i)/(1 - \hat{\pi}_i)$ in equation 12 and the quantity $Y_i(1 - D_i)/(1 - \hat{\pi}_i)$ in equation 13 with regression estimates $1 - \hat{\mu}_0$ and $\hat{\mu}_0$, respectively (derivation in Supplementary Material).

7 Inference for new unfairness measures

In this section we propose procedures for assessing the extent of unfairness according to our new metrics. The *unfairness value* that we propose is a high-level comparison between a measurement on one of our new metrics and a hypothetical, perfectly fair model. We propose approaches for estimation of standard errors and confidence intervals to provide further insight into the extent of unfairness.

7.1 An unfairness value

To assess the overall unfairness of a model, we propose an *unfairness value* (“*u-value*”), which assesses a model against a reference distribution representing a hypothetical, perfectly fair model. To construct the reference distribution, we jointly permute the protected characteristic vectors, \mathbf{A}_i , $i = 1, \dots, n$, in the observed data while holding all other data constant. The permutation simulates a situation in which protected characteristics are randomly assigned and thus have no relation to model error rates, i.e. a situation of

no unfairness. Since, even with a relatively small sample, the total number of possible permutations of the protected characteristic vectors will be large, we use Monte Carlo approximation and sample with replacement from the set of all possible permutations. We then obtain reference distributions for the metrics in Section 3 by calculating each metric on each of the permuted datasets.

Define the *u-value*, $u(S)$, of each metric as the proportion of permutations where the metric is less than its observed value in the original data. A higher u-value indicates a more extreme observed metric relative to the reference distribution, i.e. more unfairness.

For example, let $\{\widehat{\Delta}_{AVG}(S)_1^*, \dots, \widehat{\Delta}_{AVG}(S)_P^*\}$ be the set of values of Δ_{AVG} calculated across P permuted datasets.

$$u_{AVG}(S) = \frac{\sum_{j=1}^P I(\widehat{\Delta}_{AVG}(S)_j^* < \widehat{\Delta}_{AVG}(S))}{P} \quad (17)$$

The u-value is mathematically similar to a traditional p-value. However, we intentionally choose another name to avoid suggesting that unfairness should be thought of in the traditional null hypothesis testing framework. First, what constitutes a “significant” or unacceptable level of unfairness is highly subjective and context-dependent. Second, we recognize that a test of statistically significant unfairness could contribute to “ethics washing” [37] potentially problematic algorithms by giving the stamp of “fair” to any model that clears the significance threshold. Instead, we recommend using the u-value as one tool alongside the others described in this section. The u-value puts the unfairness metric in context by comparing to a hypothetical fair model, while our other inference tools describe the actual value of the metric.

7.2 Standard errors

Next we obtain standard errors for each of our new metrics. Because our metrics aggregate absolute values of error rate differences, standard bootstrap methods for obtaining standard errors cannot be used. This is because the null value for each metric is zero (corresponding to the null hypothesis of no unfairness), but zero is on the boundary of the parameter space for our metrics which take the average, maximum, or standard deviation of absolute values. It has been established that the standard bootstrap is inconsistent when the true value of the parameter is on the boundary [3]. Thus, for any model that is close to fair, using the standard bootstrap with our methods gives incorrect results.

A note on the use of absolute values: It may seem preferable to remove the absolute values and instead aggregate signed error rate differences, thus avoiding the boundary issue. However, this approach could result in cancellation of differences and underestimation of unfairness since we include each pairwise comparison only once without regard to the order of groups being compared. Aggregating positive and negative differences, when the sign is due only to the ordering, would distort our metrics. Thus we maintain the absolute values and pursue alternative inference methods.

7.2.1 Rescaled bootstrap

Instead of the standard bootstrap, we propose use of the *rescaled bootstrap* [3], also known as the *m out of n bootstrap* [7].

The rescaled bootstrap has developed as a solution to cases in which standard bootstrap estimates are inconsistent, including when the null value is on the boundary of the parameter space. The general idea is that rather than drawing bootstrap resamples of size n , where n is the sample size used to obtain the parameter estimate, we draw bootstrap

samples of size m , with $m \ll n$. The distribution of $\sqrt{m}(\hat{\theta}_m^* - \hat{\theta}_n)$ is then used to approximate the distribution of $\sqrt{n}(\hat{\theta}_n - \theta)$. where $\hat{\theta}_n$ is the parameter estimate based on n observations, $\hat{\theta}_m^*$ is a bootstrap estimate from a resample of size m , and θ is the true parameter value. Rules for the choice of m are not well established [3]; we choose $m = 0.75$ to achieve consistency while maintaining adequate sample size in the bootstrap resamples.

Let $\hat{\theta}_i^*$ be the rescaled bootstrap estimates, such that $\hat{\theta}_i^* = \sqrt{m}(\hat{\theta}_{m,i}^* - \hat{\theta}_n)$, $i = 1, \dots, B$ where B is the number of bootstrap resamples. Let $\bar{\theta}_m^*$ be the sample mean of the $\hat{\theta}_i^*$. Then we estimate the standard error of $\hat{\theta}_n$ as follows. First, take the sample variance of the rescaled bootstrap estimates. This sample variance consistently estimates the variance of $\sqrt{n}(\hat{\theta}_n - \theta)$. Then multiply by $1/n$ to obtain an estimate of the variance of $\hat{\theta}_n$. The rescaled bootstrap estimate of $SE(\hat{\theta}_n)$ is therefore:

$$\widehat{SE}(\hat{\theta}_n) = \sqrt{\frac{1}{n} \left[\frac{\sum_{i=1}^m (\hat{\theta}_i^* - \bar{\theta}_m^*)^2}{m - 1} \right]} \quad (18)$$

7.3 Confidence intervals

Using the rescaled bootstrap, we have several options for construction of confidence intervals. We propose an adaptation of the *bootstrap t-interval* adjusted for the rescaling of the bootstrap estimates. In the standard bootstrap case, the bootstrap t-interval uses the distribution of $t^* = (\hat{\theta}^* - \hat{\theta})/\hat{\sigma}^*$ to approximate the distribution of $t = (\hat{\theta} - \theta)/\hat{\sigma}$, where $\hat{\sigma}$ is an estimate of the standard deviation of $\hat{\theta}$ [8]. For the rescaled case, we obtain the values $t_m^* = (\hat{\theta}_m^* - \hat{\theta}_n)/\widehat{SE}(\hat{\theta}_n)$, using our estimate of the standard error of $\hat{\theta}$ in equation 18. Denote the empirical distribution function of the t_m^* as \hat{F}_{t^*} . Then a rescaled $1 - \alpha$ bootstrap t-interval for $\hat{\theta}_n$ is given by:

$$\left\{ \hat{\theta}_n - \widehat{SE}(\hat{\theta}_n) \hat{F}_{t^*}^{-1}(1 - \alpha/2), \hat{\theta}_n - \widehat{SE}(\hat{\theta}_n) \hat{F}_{t^*}^{-1}(\alpha/2) \right\} \quad (19)$$

We also consider for comparison two alternative methods for computing confidence intervals for $\hat{\theta}_n$ using the rescaled bootstrap.

The *normal approximation interval* uses the standard error estimate of equation 18, with $\phi^{-1}(\alpha)$ denoting the α quantile of the standard normal distribution.

$$\left\{ \hat{\theta}_n \pm \Phi^{-1}(1 - \alpha/2) \widehat{SE}(\hat{\theta}_n) \right\} \quad (20)$$

The *percentile interval* uses percentiles of the rescaled bootstrap estimates, transformed back to the scale of the parameter estimate:

$$\left\{ \frac{1}{\sqrt{m}} \hat{F}_{\theta^*}^{-1}(\alpha/2) + \hat{\theta}_n, \frac{1}{\sqrt{m}} \hat{F}_{\theta^*}^{-1}(1 - \alpha/2) + \hat{\theta}_n \right\} \quad (21)$$

where F_{θ^*} is the empirical distribution function of the rescaled bootstrap estimates $\hat{\theta}_i^*$.

We note that, of the three alternatives presented in this section, only the t-interval and normal approximation intervals can cross zero. This is because the endpoints of the percentile interval are un-centered and un-scaled rescaled bootstrap estimates, meaning they are on the original scale of the unfairness metrics which, because they aggregate absolute values, are strictly non-negative.

8 Simulations

We simulate three scenarios with varying types of unfairness to demonstrate properties of our new metrics and estimators. The first scenario simulates low unfairness, with approximately equal counterfactual error rates for all protected groups. The second scenario

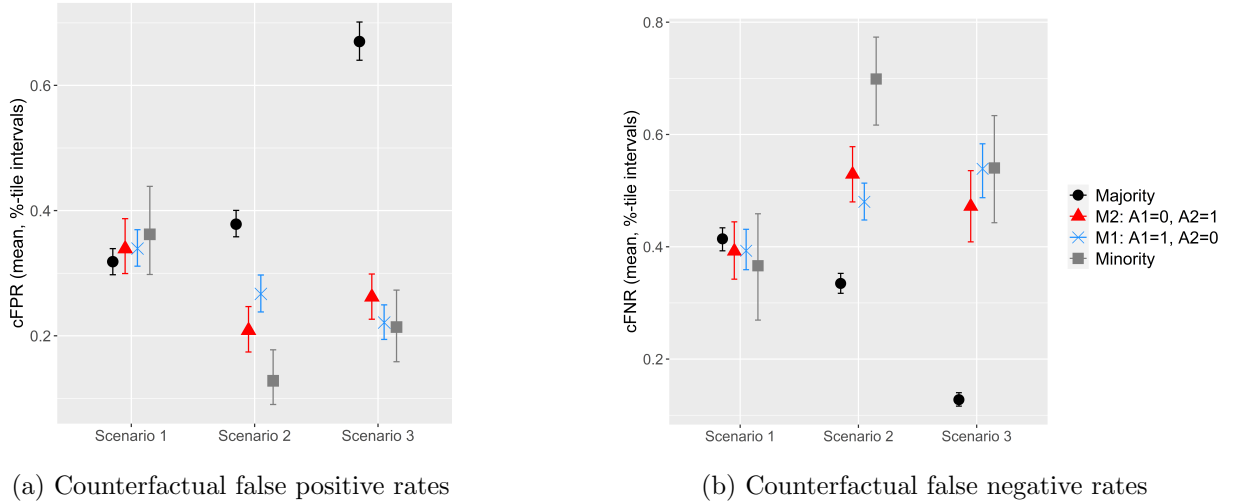


Figure 2: Counterfactual error rates by protected group for each of the unfairness scenarios considered in Section 8. Shapes show the mean of 500 replications of the estimation procedure, with $N_{estimation} = 9,000$ and the GLM propensity score model estimation method. Intervals show the 0.025 and 0.975 quantiles of the replications.

simulates unfairness involving many groups. The third scenario simulates unfairness in which one protected group has a large error rate difference with all other groups.

For all scenarios, we follow the framework used in the simulations in Section 3, in which we consider two binary protected characteristics, A_1 and A_2 . The group with $A_1 = 1, A_2 = 1$ is the numeric minority, and the group with $A_1 = 0, A_2 = 0$ is the majority group. We refer to the two other groups as $M1$ and $M2$ by the characteristic (A_1 or A_2) which is equal to 1. Figure 2 depicts the three scenarios in terms of counterfactual false positive ($cFPR$) and false negative ($cFNR$) rates. In the first scenario, the model performs nearly identically for all groups. The second scenario shows more differences, with the minority group having the lowest $cFPR$ (Figure 2a) and highest $cFNR$ (Figure 2b), and the majority group having the reverse.. In the third scenario, the majority group has a substantially higher $cFPR$ (and lower $cFNR$) than all other groups.

8.1 Data generation and simulation set-up

The foundation for our simulations is the data generating procedure described in [29], in which a training data set is generated as the basis for training a risk prediction model. Our training data set is of size $N_{train} = 1,000$, and our risk prediction model is a random forest. We then generate a validation data set with sample size 50,000 to establish the true error rate properties of the risk model. As noted in [29], because we have control over the entire data generation process, we know the potential outcomes Y^0 for all observations in this validation set. Thus we can determine the “true” values of the counterfactual error rates and unfairness metrics. Finally, we generate what we refer to as the “estimation” data set. We obtain binary risk predictions on this data using the risk prediction model and a classification cutoff of 0.5. We then perform nuisance parameter estimation and estimate the values of our unfairness metrics. Full details of the data generating process and scenarios are given in the Supplementary Material.

For each of our three unfairness scenarios, we consider three estimation data set sample sizes (1,000, 5,000, 7,000, 9,000). We consider the four estimation methods described in Section 6: regression estimation and inverse probability weighting using three propensity score models (GLM, ensemble, true data generating mechanism). For the ensemble propensity score model, we use a super learner combining a generalized linear model and a random forest. The regression estimates use a generalized linear model. We perform 500 replications of the data set generation and estimation procedure for each combination of parameters and unfairness scenario.

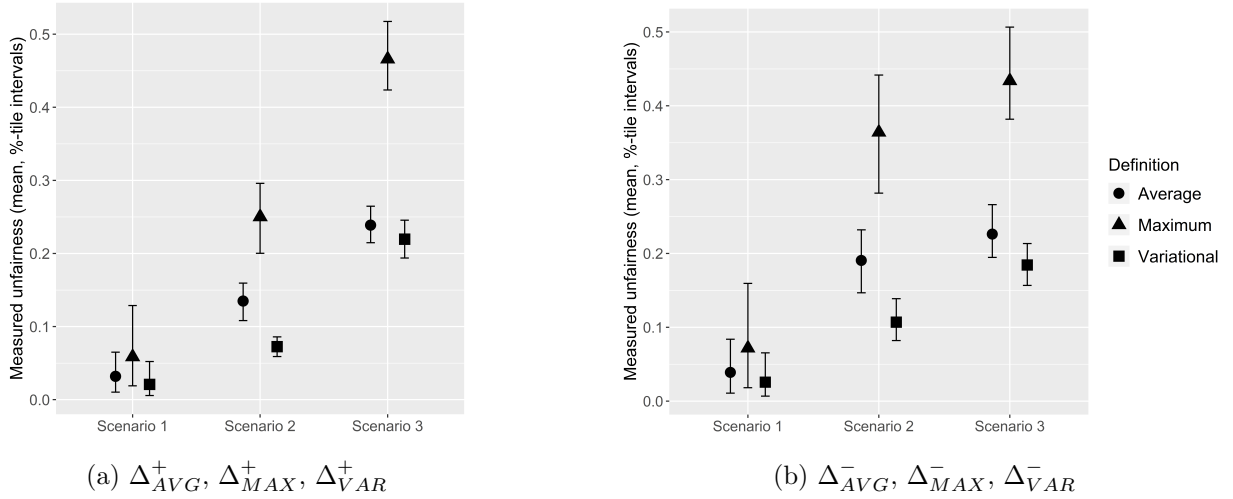


Figure 3: Comparisons of positive (left) and negative (right) versions of new metrics. Shapes show the mean of 500 replications of the estimation procedure, with $N_{estimation} = 9,000$ and the GLM propensity score model estimation method. Intervals show the 0.025 and 0.975 quantiles of the replications.

8.2 Comparison of novel unfairness metrics

This section compares our new unfairness metrics using a slightly more realistic data generating scenario than the simple example in Section 4.

In Scenario 1, with little unfairness, the three metrics are clustered together at a low value in both their positive (Figure 3a) and negative (Figure 3b) versions. In Scenario 2, differences emerge between Δ_{AVG} and Δ_{VAR} , with the relatively lower value of Δ_{VAR} reflecting more even spacing of the error rates compared to Scenario 3. In this scenario, Δ_{MAX} is larger to reflect the large error rate differences between the minority and $M2$ and the other two groups. In Scenario 3, Δ_{MAX} is even larger because of the larger error rate differences between the majority and all other groups. However, Δ_{AVG} and Δ_{VAR} are closer together because the error rates are less evenly spaced.

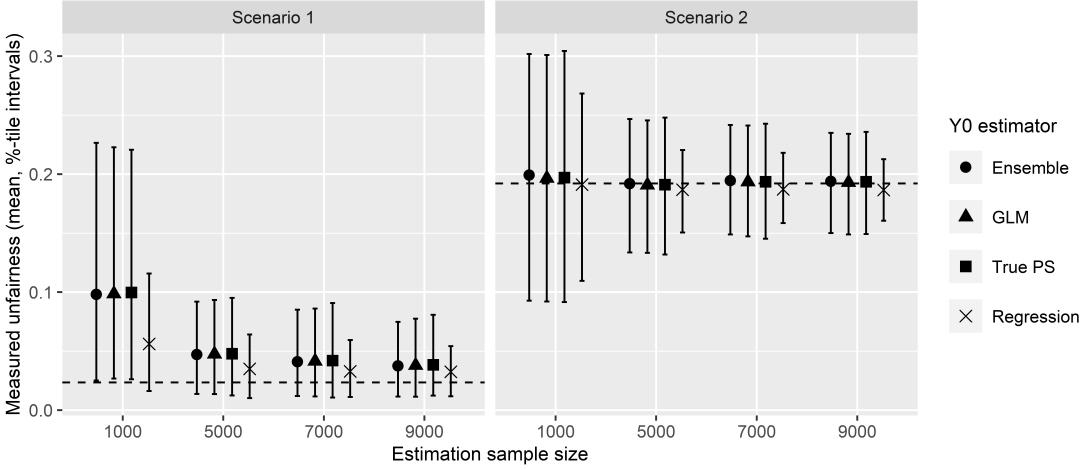


Figure 4: Performance of estimation methods for the negative version of Δ_{AVG} under Scenario 1 (low unfairness) and Scenario 2 (more unfairness). Shapes show the mean of 500 replications of the estimation procedure, and error bars show the 0.025 and 0.975 quantiles. The true values, as obtained from the validation data sets for each scenario, are shown with the horizontal dotted lines. Estimation methods considered are the regression estimator (“Regression”) and weighted estimators using ensemble and GLM propensity score models. A weighted estimator using the true propensity score model (“True PS”) is included for comparison.

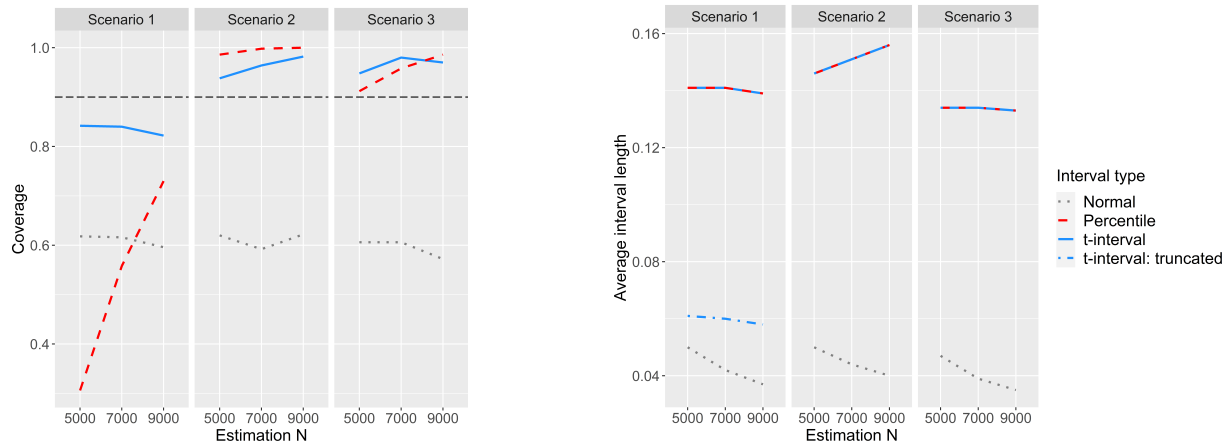
8.3 Comparison of estimation methods

Figure 4 demonstrates the performance of the estimation methods proposed in Section 6. We focus on the negative version of Δ_{AVG} and show scenarios 1 and 2 to demonstrate performance with both near-zero and higher unfairness. As the estimation sample size increases, the precision of the estimates increases for all methods and scenarios, as shown by the decreasing lengths of the error bars. In Scenario 1 (low unfairness), all methods overestimate the true unfairness at low sample sizes, but all methods approach the correct value as the sample size increases. For this data, in which the true data generating mechanism is known and the regression estimator can be correctly specified, it performs slightly better than the weighted estimators at lower sample sizes.

In Scenario 2 (more unfairness), all methods correctly approximate the true value at all sample sizes. Again, with the regression model correctly specified, it returns slightly

shorter intervals than the weighted methods.

8.4 Inference



(a) Coverage rates of 90% confidence intervals for $\widehat{\Delta}_{AVG}^-$ using three methods.

(b) Average length of 90% confidence intervals for $\widehat{\Delta}_{AVG}^-$ using three methods.

Figure 5: Lines show the performance of three methods for estimating confidence intervals for our proposed metrics, all using GLM propensity score estimation. Methods shown are normal approximation (dotted), percentile (dashed), and t-interval (solid). For each combination of scenario and sample size, coverage rates and average length of the 90% confidence intervals are calculated using 1,000 rescaled bootstrap resamples on each of 500 estimation data sets. The horizontal dashed line in the Figure 5a shows the nominal coverage rate of 90%. The average length of the t-intervals truncated at zero is also shown, since only the non-negative portion indicates plausible values for $\widehat{\Delta}_{AVG}^-$.

Figure 5 shows the performance of several methods for constructing confidence intervals using the rescaled bootstrap, again focusing on the negative version of Δ_{AVG} . Of the three methods, only the t-interval has coverage close to the nominal rate in Scenario 1 (low unfairness) at smaller sample sizes. All methods except the normal approximation have coverage above the nominal rate in Scenarios 2 and 3 (more unfairness). Increasing sample size improves coverage for all methods and most dramatically for the percentile interval. The normal approximation gives the shortest intervals in all scenarios. The percentile and t-interval methods give intervals of the same length; however, when the t-intervals are

truncated at zero in Scenario 1, their length is more comparable to that of the normal intervals. In Scenarios 2 and 3, truncation has no effect since the t-intervals do not cross zero. Increasing sample size shortens intervals in most cases, except the percentile and t-interval in Scenario 2.

9 Demonstration of proposed framework

This section demonstrates our estimation and inference framework as it would be applied to evaluate a risk model. We focus on Scenarios 1 and 2 described in Section 8 to demonstrate application to more and less fair models.

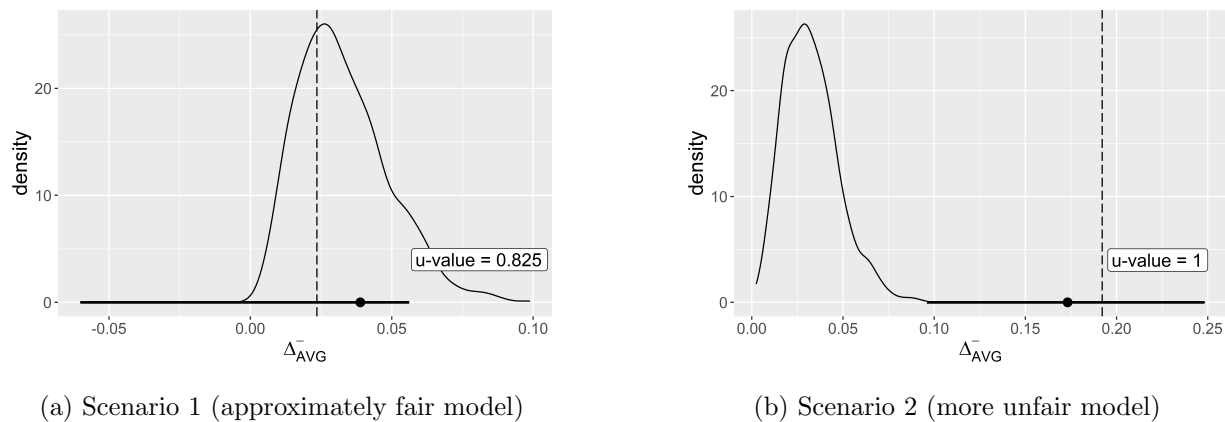


Figure 6: Demonstration of estimation and inference techniques for Δ_{AVG}^- . Dots and solid segments on the x-axis show estimated values and 90% confidence intervals. Density plot shows the reference distribution, from which the u-value is obtained as the proportion of reference distribution estimates of Δ_{AVG}^- that are less than or equal to the observed value.

First, estimates of each of the novel metrics, Δ_{AVG} , Δ_{MAX} , and Δ_{VAR} , are calculated on the observed data. We then employ the reference distribution method of Section 7.1, obtaining distributions and calculating corresponding u-values for each of the three metrics. Finally, we follow the standard error and confidence interval procedures of Sections 7.2.1 and 7.3.

Results for the *cFNR* version of our Average metric (Δ_{AVG}^-) show that in Scenario 1

(Figure 6a), with minimal unfairness, the estimated value (dot on x-axis) is small, and the 90% confidence interval (solid segment) contains zero. The reference distribution is shown with the density plot; in this situation of low unfairness, the true value (vertical dotted line) is in the middle of the distribution, showing that this model is, in fact, approximately fair on the Δ_{AVG}^- metric. Our estimated value and interval also sit in the middle of the reference distribution. The u-value is 0.825, meaning about 18 percent of reference distribution estimates were more extreme than the observed value. These results indicate minimal unfairness on the Δ_{AVG}^- metric in this scenario.

In Scenario 2, with more unfairness, the estimated value and confidence interval are much farther in the right tail of the reference distribution (Figure 6b). The u-value is 1, meaning no reference distribution estimates were greater than the observed value. These results indicate the presence of unfairness according to the Δ_{AVG}^- metric. Upon obtaining this type of result, the next step for practitioners would be to look at all three of our proposed metrics together to learn about the size and spread of error rate differences as described in Section 4 and to examine group-specific error rates and associated confidence intervals in a plot similar to Figure 2.

10 Discussion

In this paper we proposed tools for measuring intersectional, counterfactual unfairness in risk prediction models. We built on work by [29], who developed the counterfactual equalized odds framework in the context of a single protected characteristic. We proposed three novel counterfactual unfairness metrics that accommodate multiple intersecting protected characteristics and are valid in contexts where a risk score is used to guide treatment. We demonstrated how multiple measures of fairness, e.g. our three new metrics, are needed

to fully diagnose a model. We defined the *unfairness value* (“*u-value*”) to summarize the overall unfairness of a model according to our metrics and developed a full set of inference tools to determine the extent of unfairness.

10.1 A wider lens for fairness

Our intersectional fairness methods advance the conversation in clinical risk prediction by providing more nuanced, realistic measurements of inequities in model performance. However, intersectional fairness as it is typically defined and as we have defined it here, e.g. a set of technical tools for assessing and correcting differential model performance across intersecting groups, does not in itself constitute an intersectional analysis according to the original meaning of the term in Black feminist scholarship. Intersectionality is about power relationships and a push toward social justice. As such, our work is just one piece of the widespread effort required for intersectional fairness in risk prediction and algorithmic processes more generally, including work at all stages of the model development and deployment process [11]. Critics of technical algorithmic fairness solutions note that an over-emphasis on these methods distracts from and can undermine work at other stages, including fairness considerations in problem selection, representation of affected groups, and implementation. Technical fairness work can also be used to “ethics wash” problematic algorithms, providing the illusion of an ethical product while distracting from more fundamental questions about whether the algorithms should be used at all [37, 25]. Rather than spend all our time mitigating bad models, [37] argues for the use of prediction to actively challenge oppression (as in, for example [40, 17]).

Nevertheless, due to both the significant potential benefits from risk prediction in health care and the fast-growing use of these tools, improved technical methods for measuring

fairness are still needed. While not the whole, fairness metrics are a part of work towards ethical machine learning in health care. Work such as [16], which outlines the core tenets of an intersectional approach to fairness measurement, may help bridge the gap between technical methods and the wider fairness picture.

10.2 Further directions for intersectional, counterfactual fairness measurement

Within our work on improved fairness measurement, several statistical issues remain for exploration. In this work we assume the availability of sufficient sample size in each intersection of the protected characteristics. When selecting characteristics, there is a trade-off between increased nuance, obtained by considering more intersecting characteristics or disaggregating categories within a characteristic, and decreased precision or inability to obtain estimates due to insufficient sample size. One solution may be to select, in a data or context-driven manner, particular combinations of protected characteristics for which to assess fairness [36]. Others have proposed methods for such selection which, while not applied to the clinical context, provide a guide for future work [30].

On the other end of the sample size spectrum, when the sample size becomes very large, the permutation null distributions of Section 7.1 become increasingly narrow and even small amounts of unfairness give u -values around 1. In these cases, the confidence interval procedure of Section 7.3 can be used to more precisely determine the magnitude of model unfairness.

Finally, while our methods can use any protected characteristics, the selection and definition of characteristics is critical to the validity of the results in context. Particularly with socially constructed characteristics like race, assignment of group labels is not straightfor-

ward, and group definitions change over time. In the case of race, existing work notes a few further specific issues. Racial categories are inherently unequal groupings used to perpetuate inequities, so [6] argues that fairness work should be careful of further entrenching the labels. They argue for using patterns of segregation, rather than racial categories, to guide fairness interventions with the goal of disrupting such patterns. Recent work on a multidimensional measure of structural racism [10] provides another potential alternative definition of categories that could be used in metrics such as ours. At a minimum, the complexities of measuring structural racism that [18] and others note suggest that group definition for algorithmic fairness work involving race deserves further study.

References

- [1] Zeeshan Aleem. *New CDC Data Shows Covid-19 Is Affecting African Americans at Exceptionally High Rates*. Vox. Apr. 18, 2020. URL: <https://www.vox.com/coronavirus-covid19/2020/4/18/21226225/coronavirus-black-cdc-infection> (visited on 09/02/2022).
- [2] Alexia Fernández Campbell. *Even with Positive Jobs Report, Latinas Still Hardest Hit by COVID-19 Slowdown. Here's Why*. Center for Public Integrity. June 5, 2020. URL: <http://publicintegrity.org/health/coronavirus-and-inequality/even-with-positive-jobs-report-latinas-still-hardest-hit-by-covid-slowdown-heres-why/> (visited on 09/02/2022).
- [3] Donald W. K. Andrews. “Inconsistency of the Bootstrap When a Parameter Is on the Boundary of the Parameter Space”. In: *Econometrica* 68.2 (2000), pp. 399–405. ISSN: 0012-9682. JSTOR: 2999432.

- [4] Julia Angwin et al. *Machine Bias*. ProPublica. URL: https://www.propublica.org/article/machine-bias-risk-assessments-in-criminal-sentencing?token=Gg58888u2U5db3W3CsuKrD0LD_VQJReQ (visited on 06/27/2020).
- [5] David W. Bates et al. “Big Data In Health Care: Using Analytics To Identify And Manage High-Risk And High-Cost Patients”. In: *Health Affairs* 33.7 (July 2014), pp. 1123–1131. ISSN: 0278-2715. DOI: 10.1377/hlthaff.2014.0041. URL: <https://www.healthaffairs.org/doi/10.1377/hlthaff.2014.0041> (visited on 03/21/2022).
- [6] Sebastian Benthall and Bruce D. Haynes. “Racial Categories in Machine Learning”. In: *Proceedings of the Conference on Fairness, Accountability, and Transparency - FAT* '19* (2019), pp. 289–298. DOI: 10.1145/3287560.3287575. arXiv: 1811.11668. URL: <http://arxiv.org/abs/1811.11668> (visited on 06/29/2020).
- [7] P. J. Bickel, F. Götze, and W. R. van Zwet. “Resampling Fewer Than n Observations: Gains, Losses, and Remedies for Losses”. In: *Statistica Sinica* 7.1 (Jan. 1997), pp. 1–31. JSTOR: 26432490.
- [8] Dennis D Boos and L. A Stefanski. *Essential Statistical Inference*. Vol. 120. Springer Texts in Statistics. New York, NY: Springer, 2013. ISBN: 978-1-4614-4818-1. DOI: 10.1007/978-1-4614-4818-1. URL: <http://link.springer.com/10.1007/978-1-4614-4818-1> (visited on 04/18/2022).
- [9] Alessandro Castelnovo et al. “A Clarification of the Nuances in the Fairness Metrics Landscape”. In: *Scientific Reports* 12.1 (Dec. 2022), p. 4209. ISSN: 2045-2322. DOI: 10.1038/s41598-022-07939-1. arXiv: 2106.00467. URL: <http://arxiv.org/abs/2106.00467> (visited on 03/22/2022).

- [10] Tongtan Chantararat, David C. Van Riper, and Rachel R. Hardeman. “The Intricacy of Structural Racism Measurement: A Pilot Development of a Latent-Class Multidimensional Measure”. In: *EClinicalMedicine* 40 (Oct. 1, 2021), p. 101092. ISSN: 2589-5370. DOI: 10.1016/j.eclinm.2021.101092. URL: <https://www.sciencedirect.com/science/article/pii/S2589537021003722> (visited on 06/24/2022).
- [11] Irene Y. Chen et al. “Ethical Machine Learning in Health Care”. Sept. 23, 2020. arXiv: 2009.10576 [cs]. URL: <http://arxiv.org/abs/2009.10576> (visited on 09/27/2020).
- [12] Amanda Coston et al. “Counterfactual Risk Assessments, Evaluation, and Fairness”. In: *Proceedings of the 2020 Conference on Fairness, Accountability, and Transparency. FAT* ’20*. New York, NY, USA: Association for Computing Machinery, Jan. 27, 2020, pp. 582–593. ISBN: 978-1-4503-6936-7. DOI: 10.1145/3351095.3372851. URL: <https://doi.org/10.1145/3351095.3372851> (visited on 09/09/2020).
- [13] Kimberle Crenshaw. “Demarginalizing the Intersection of Race and Sex: A Black Feminist Critique of Antidiscrimination Doctrine, Feminist Theory and Antiracist Politics”. In: *University of Chicago Legal Forum* 1989.1 (1989), p. 31.
- [14] Kimberle Crenshaw. “Mapping the Margins: Intersectionality, Identity Politics, and Violence against Women of Color”. In: *Stanford Law Review* 43.6 (1991), pp. 1241–1299. ISSN: 0038-9765. DOI: 10.2307/1229039. JSTOR: 1229039.
- [15] Jake Fawkes, Robin Evans, and Dino Sejdinovic. “Selection, Ignorability and Challenges With Causal Fairness”. Feb. 28, 2022. arXiv: 2202.13774 [cs, stat]. URL: <http://arxiv.org/abs/2202.13774> (visited on 03/01/2022).
- [16] James R. Foulds et al. “An Intersectional Definition of Fairness”. In: *2020 IEEE 36th International Conference on Data Engineering (ICDE)*. 2020 IEEE 36th Interna-

- tional Conference on Data Engineering (ICDE). Dallas, TX, USA: IEEE, Apr. 2020, pp. 1918–1921. ISBN: 978-1-72812-903-7. DOI: 10.1109/ICDE48307.2020.00203. URL: <https://ieeexplore.ieee.org/document/9101635/> (visited on 05/06/2021).
- [17] Sharad Goel, Justin M. Rao, and Ravi Shroff. “Precinct or Prejudice? Understanding Racial Disparities in New York City’s Stop-and-Frisk Policy”. In: *The Annals of Applied Statistics* 10.1 (Mar. 2016), pp. 365–394. ISSN: 1932-6157, 1941-7330. DOI: 10.1214/15-A0AS897. URL: <https://projecteuclid.org/journals/annals-of-applied-statistics/volume-10/issue-1/Precinct-or-prejudice-Understanding-racial-disparities-in-New-York-Citys/10.1214/15-A0AS897.full> (visited on 06/24/2022).
- [18] Rachel R. Hardeman et al. “Improving The Measurement Of Structural Racism To Achieve Antiracist Health Policy”. In: *Health Affairs* 41.2 (Feb. 2022), pp. 179–186. ISSN: 0278-2715. DOI: 10.1377/hlthaff.2021.01489. URL: <http://www.healthaffairs.org/doi/full/10.1377/hlthaff.2021.01489> (visited on 09/05/2022).
- [19] Ursula Hebert-Johnson et al. “Multicalibration: Calibration for the (Computationally-Identifiable) Masses”. In: *International Conference on Machine Learning*. International Conference on Machine Learning. PMLR, July 3, 2018, pp. 1939–1948. URL: <http://proceedings.mlr.press/v80/hebert-johnson18a.html> (visited on 05/10/2021).
- [20] Patricia Hill Collins. “Intersectionality’s Definitional Dilemmas”. In: *Annual Review of Sociology* 41.1 (Aug. 14, 2015), pp. 1–20. ISSN: 0360-0572, 1545-2115. DOI: 10.1146/annurev-soc-073014-112142. URL: <https://www.annualreviews.org/doi/10.1146/annurev-soc-073014-112142> (visited on 03/16/2022).

- [21] Patricia Hill Collins and Sirma Bilge. *Intersectionality*. Cambridge, UK: Polity Press, June 13, 2016. ISBN: 978-0-7456-8452-9. URL: <http://ebookcentral.proquest.com/lib/umn/detail.action?docID=4698012> (visited on 01/18/2022).
- [22] Intersectionality Training Institute. *What Is Intersectionality?* Intersectionality Training Institute. URL: <https://www.intersectionalitytraining.org/intersectionality-basics> (visited on 03/16/2022).
- [23] Michael Kearns et al. “Preventing Fairness Gerrymandering: Auditing and Learning for Subgroup Fairness”. In: *International Conference on Machine Learning*. International Conference on Machine Learning. PMLR, July 3, 2018, pp. 2564–2572. URL: <http://proceedings.mlr.press/v80/kearns18a.html> (visited on 05/10/2021).
- [24] Arman Kilic. “Artificial Intelligence and Machine Learning in Cardiovascular Health Care”. In: *The Annals of Thoracic Surgery* 109.5 (May 1, 2020), pp. 1323–1329. ISSN: 0003-4975. DOI: 10.1016/j.athoracsur.2019.09.042. URL: <https://www.sciencedirect.com/science/article/pii/S0003497519316121> (visited on 03/21/2022).
- [25] Youjin Kong. “Are “Intersectionally Fair” AI Algorithms Really Fair to Women of Color? A Philosophical Analysis”. In: *2022 ACM Conference on Fairness, Accountability, and Transparency*. FAccT ’22: 2022 ACM Conference on Fairness, Accountability, and Transparency. Seoul Republic of Korea: ACM, June 21, 2022, pp. 485–494. ISBN: 978-1-4503-9352-2. DOI: 10.1145/3531146.3533114. URL: <https://dl.acm.org/doi/10.1145/3531146.3533114> (visited on 06/23/2022).
- [26] Matt J Kusner et al. “Counterfactual Fairness”. In: *NeurIPS Proceedings*. 31st Conference on Neural Information Processing System. Long Beach, CA, p. 11.

- [27] Mark J. van der Laan, Eric C. Polley, and Alan E. Hubbard. “Super Learner”. In: *Statistical Applications in Genetics and Molecular Biology* 6.1 (Sept. 16, 2007). ISSN: 1544-6115. DOI: 10.2202/1544-6115.1309. URL: <http://www.degruyter.com/document/doi/10.2202/1544-6115.1309/html> (visited on 09/12/2022).
- [28] Melanie Evans and Anna Wilde Mathews. “New York Regulator Probes United-Health Algorithm for Racial Bias”. In: *Wall Street Journal. US* (Oct. 26, 2019). ISSN: 0099-9660. URL: <https://www.wsj.com/articles/new-york-regulator-probes-unitedhealth-algorithm-for-racial-bias-11572087601> (visited on 10/06/2021).
- [29] Alan Mishler, Edward H. Kennedy, and Alexandra Chouldechova. “Fairness in Risk Assessment Instruments: Post-Processing to Achieve Counterfactual Equalized Odds”. In: *Proceedings of the 2021 ACM Conference on Fairness, Accountability, and Transparency* (Mar. 3, 2021), pp. 386–400. DOI: 10.1145/3442188.3445902. arXiv: 2009.02841. URL: <http://arxiv.org/abs/2009.02841> (visited on 11/17/2021).
- [30] Mathieu Molina and Patrick Loiseau. *Bounding and Approximating Intersectional Fairness through Marginal Fairness*. June 12, 2022. DOI: 10.48550/arXiv.2206.05828. arXiv: 2206.05828 [cs, stat]. URL: <http://arxiv.org/abs/2206.05828> (visited on 06/15/2022).
- [31] Giulio Morina et al. *Auditing and Achieving Intersectional Fairness in Classification Problems*. June 8, 2020. DOI: 10.48550/arXiv.1911.01468. URL: <https://arxiv.org/abs/1911.01468>.
- [32] Sara G Murray, Robert M Wachter, and Russell J Cucina. *Discrimination By Artificial Intelligence In A Commercial Electronic Health Record—A Case Study — Health*

- Affairs Blog*. Health Affairs Blog. Jan. 31, 2020. URL: <https://www.healthaffairs.org/doi/10.1377/hblog20200128.626576/full/> (visited on 01/09/2021).
- [33] Jennifer C. Nash. *Black Feminism Reimagined: After Intersectionality*. Next Wave (Duke University Press). Durham: Duke University Press, 2019. ISBN: 978-1-4780-0059-4.
- [34] Ziad Obermeyer et al. “Dissecting Racial Bias in an Algorithm Used to Manage the Health of Populations”. In: *Science* 366.6464 (Oct. 25, 2019), pp. 447–453. DOI: 10.1126/science.aax2342. URL: <https://www.science.org/doi/full/10.1126/science.aax2342> (visited on 10/12/2021).
- [35] Donald B. Rubin. “Statistics and Causal Inference: Comment: Which Ifs Have Causal Answers”. In: *Journal of the American Statistical Association* 81.396 (Dec. 1986), p. 961. ISSN: 01621459. DOI: 10.2307/2289065. JSTOR: 2289065.
- [36] Angelina Wang, Vikram V. Ramaswamy, and Olga Russakovsky. *Towards Intersectionality in Machine Learning: Including More Identities, Handling Underrepresentation, and Performing Evaluation*. May 9, 2022. DOI: 10.1145/3531146.3533101. arXiv: 2205.04610 [cs]. URL: <http://arxiv.org/abs/2205.04610> (visited on 05/19/2022).
- [37] Lindsay Weinberg. “Rethinking Fairness: An Interdisciplinary Survey of Critiques of Hegemonic ML Fairness Approaches”. In: *Journal of Artificial Intelligence Research* 74 (May 6, 2022), pp. 75–109. ISSN: 1076-9757. DOI: 10.1613/jair.1.13196. arXiv: 2205.04460. URL: <http://arxiv.org/abs/2205.04460> (visited on 05/12/2022).
- [38] Forest Yang, Mouhamadou Cisse, and Sanmi Koyejo. “Fairness with Overlapping Groups; a Probabilistic Perspective”. In: *Advances in Neural Information Processing Systems* 33 (2020), pp. 4067–4078. URL: <https://proceedings.neurips.cc/>

paper/2020/hash/29c0605a3bab4229e46723f89cf59d83-Abstract.html (visited on 05/06/2021).

- [39] Ke Yang, Joshua R. Loftus, and Julia Stoyanovich. “Causal Intersectionality for Fair Ranking”. In: (June 15, 2020). URL: <https://arxiv.org/abs/2006.08688v1> (visited on 05/06/2021).
- [40] Teng Ye et al. “Using Machine Learning to Help Vulnerable Tenants in New York City”. In: *Proceedings of the Conference on Computing & Sustainable Societies - COMPASS 19*. The 2nd ACM SIGCAS Conference. Accra, Ghana: ACM Press, 2019, pp. 248–258. ISBN: 978-1-4503-6714-1. DOI: 10.1145/3314344.3332484. URL: <http://dl.acm.org/citation.cfm?doid=3314344.3332484> (visited on 08/14/2021).
- [41] Zhe Yu. “Fair Balance: Mitigating Machine Learning Bias Against Multiple Protected Attributes With Data Balancing”. July 17, 2021. arXiv: 2107.08310 [cs]. URL: <http://arxiv.org/abs/2107.08310> (visited on 09/20/2021).

11 Supplementary Material

11.1 Proofs and derivations

11.1.1 Proof of Proposition 1

Let D denote a binary treatment assignment, S a binary risk prediction, \mathbf{A} a protected characteristic vector, and Y^0 the binary potential outcome under no treatment. Define the propensity score function for a given set of protected characteristics as $\pi = \mathbb{P}(D = 1|\mathbf{A}, \mathbf{X}, S)$.

Then the following holds for functions $f(S)$ and $g(Y^0)$:

$$\begin{aligned}
 E[f(S)g(Y^0)I(\mathbf{A} = \mathbf{a})] &= E \left[\frac{Pr(D = 0|\mathbf{A}, \mathbf{X}, S)}{Pr(D = 0|\mathbf{A}, \mathbf{X}, S)} f(S)g(Y^0)I(\mathbf{A} = \mathbf{a}) \right] \\
 &= E \left[\frac{1}{1 - \pi(\mathbf{A}, \mathbf{X}, S)} f(S)g(Y^0)I(\mathbf{A} = \mathbf{a})E(1 - D|\mathbf{A}, \mathbf{X}, S) \right] \\
 &= E \left[\frac{1}{1 - \pi(\mathbf{A}, \mathbf{X}, S)} f(S)g(Y^0)I(\mathbf{A} = \mathbf{a})E(1 - D|Y^0, \mathbf{A}, \mathbf{X}, S) \right]
 \end{aligned} \tag{22}$$

$$= E \left\{ E \left[\frac{(1 - D)f(S)g(Y^0)I(\mathbf{A} = \mathbf{a})}{1 - \pi(\mathbf{A}, \mathbf{X}, S)} \middle| Y^0, \mathbf{A}, \mathbf{X}, S \right] \right\}$$

$$= E \left[\frac{(1 - D)f(S)g(Y^0)I(\mathbf{A} = \mathbf{a})}{1 - \pi(\mathbf{A}, \mathbf{X}, S)} \right] \tag{23}$$

$$= E \left[\frac{(1 - D)f(S)g(Y)I(\mathbf{A} = \mathbf{a})}{1 - \pi(\mathbf{A}, \mathbf{X}, S)} \right] \tag{24}$$

Line 22 follows from assumption A3 (Ignorability). Line 23 follows from the law of total expectation, and line 24 follows from assumption A1 (Consistency).

We then write each of the counterfactual error rates in terms of the functions $f(\cdot)$ and $g(\cdot)$ and apply the preceding result.

11.1.2 Derivation of counterfactual false positive rate

$$\begin{aligned}
cFPR(S, \mathbf{a}) &= Pr(S = 1 | Y^0 = 0, \mathbf{A} = \mathbf{a}) \\
&= \frac{Pr(S = 1, Y^0 = 0, \mathbf{A} = \mathbf{a})}{Pr(Y^0 = 0, \mathbf{A} = \mathbf{a})} \\
&= \frac{E[I(S = 1)I(Y^0 = 0)I(\mathbf{A} = \mathbf{a})]}{E[I(Y^0 = 0)I(\mathbf{A} = \mathbf{a})]} \\
&= \frac{E[S(1 - Y^0)I(\mathbf{A} = \mathbf{a})]}{E[(1 - Y^0)I(\mathbf{A} = \mathbf{a})]} \\
&= \frac{E\left[\frac{(1-D)S(1-Y)I(\mathbf{A}=\mathbf{a})}{1-\pi(\mathbf{A},\mathbf{X},S)}\right]}{E\left[\frac{(1-D)(1-Y)I(\mathbf{A}=\mathbf{a})}{1-\pi(\mathbf{A},\mathbf{X},S)}\right]}
\end{aligned}$$

where the last line follows from Proposition 1 with $f(S) = S$ and $g(Y^0) = 1 - Y^0$.

11.1.3 Derivation of counterfactual false negative rate

$$\begin{aligned}
cFNR(S, \mathbf{a}) &= Pr(S = 0 | Y^0 = 1, \mathbf{A} = \mathbf{a}) \\
&= \frac{Pr(S = 0, Y^0 = 1, \mathbf{A} = \mathbf{a})}{Pr(Y^0 = 1, \mathbf{A} = \mathbf{a})} \\
&= \frac{E[I(S = 0)I(Y^0 = 1)I(\mathbf{A} = \mathbf{a})]}{E[I(Y^0 = 1)I(\mathbf{A} = \mathbf{a})]} \\
&= \frac{E[(1 - S)Y^0 I(\mathbf{A} = \mathbf{a})]}{E[Y^0 I(\mathbf{A} = \mathbf{a})]} \\
&= \frac{E\left[\frac{(1-D)(1-S)YI(\mathbf{A}=\mathbf{a})}{1-\pi(\mathbf{A},\mathbf{X},S)}\right]}{E\left[\frac{(1-D)YI(\mathbf{A}=\mathbf{a})}{1-\pi(\mathbf{A},\mathbf{X},S)}\right]}
\end{aligned}$$

where the last line follows from Proposition 1 with $f(S) = 1 - S$ and $g(Y^0) = Y^0$.

11.1.4 Derivation for regression estimators of $cFPR(S, \mathbf{a})$ and $cFNR(S, \mathbf{a})$

$$\begin{aligned}
cFPR(S, \mathbf{a}) &= \frac{Pr(S = 1, Y^0 = 0, \mathbf{A} = \mathbf{a})}{Pr(Y^0 = 0, \mathbf{A} = \mathbf{a})} \\
&= \frac{E[Pr(S = 1, Y^0 = 0, \mathbf{A} = \mathbf{a} | \mathbf{X})]}{E[Pr(Y^0 = 0, \mathbf{A} = \mathbf{a} | \mathbf{X})]} \\
&= \frac{E[Pr(Y^0 = 0 | S = 1, \mathbf{A} = \mathbf{a}, \mathbf{X}) Pr(S = 1, \mathbf{A} = \mathbf{a} | \mathbf{X})]}{E[Pr(Y^0 = 0 | \mathbf{A} = \mathbf{a}, \mathbf{X}) Pr(\mathbf{A} = \mathbf{a} | \mathbf{X})]} \\
&= \frac{E[Pr(Y = 0 | S = 1, \mathbf{A} = \mathbf{a}, \mathbf{X}, D = 0) Pr(S = 1, \mathbf{A} = \mathbf{a} | \mathbf{X})]}{E[Pr(Y = 0 | \mathbf{A} = \mathbf{a}, \mathbf{X}, D = 0) Pr(\mathbf{A} = \mathbf{a} | \mathbf{X})]} \tag{25} \\
&= \frac{E[1 - E[Y | S = 1, \mathbf{A} = \mathbf{a}, \mathbf{X}, D = 0] E[I(\mathbf{A} = \mathbf{a}) S | \mathbf{X}]]}{E[1 - E[Y | \mathbf{A} = \mathbf{a}, \mathbf{X}, D = 0] E[I(\mathbf{A} = \mathbf{a}) | \mathbf{X}]]} \\
&= \frac{E[1 - E[Y | S = 1, \mathbf{A} = \mathbf{a}, \mathbf{X}, D = 0] I(\mathbf{A} = \mathbf{a}) S]}{E[1 - E[Y | \mathbf{A} = \mathbf{a}, \mathbf{X}, D = 0] I(\mathbf{A} = \mathbf{a})]}
\end{aligned}$$

where line 25 follows from assumption A1 (Consistency).

To estimate this quantity, define $\mu_0(\mathbf{X}, \mathbf{A}, S) = E[Y | \mathbf{X}, \mathbf{A}, S, D = 0]$ and $\mu_0^*(\mathbf{X}, \mathbf{A}) = E[Y | \mathbf{X}, \mathbf{A}, D = 0]$. We model these quantities with generalized linear models and denote the estimated probabilities $\hat{\mu}_0$ and $\hat{\mu}_0^*$. Then the regression estimator for the counterfactual false positive rate is:

$$\widehat{cFPR}(S, \mathbf{a}) = \frac{\sum_{i=1}^n 1 - \hat{\mu}_0(\mathbf{X}_i, \mathbf{A}_i, S = 1) S_i I(\mathbf{A}_i = \mathbf{a})}{\sum_{i=1}^n 1 - \hat{\mu}_0^*(\mathbf{X}_i, \mathbf{A}_i) I(\mathbf{A}_i = \mathbf{a})}$$

The regression estimator for the counterfactual false negative rate is obtained similarly:

$$\begin{aligned}
cFNR(S, \mathbf{a}) &= \frac{Pr(S = 0, Y^0 = 1, \mathbf{A} = \mathbf{a})}{Pr(Y^0 = 1, \mathbf{A} = \mathbf{a})} \\
&= \frac{E[Pr(S = 0, Y^0 = 1, \mathbf{A} = \mathbf{a}) | \mathbf{X}]}{E[Pr(Y^0 = 1, \mathbf{A} = \mathbf{a}) | \mathbf{X}]} \\
&= \frac{E[Pr(Y = 1 | S = 0, \mathbf{A} = \mathbf{a}, \mathbf{X}, D = 0) Pr(S = 0, \mathbf{A} = \mathbf{a} | \mathbf{X})]}{E[Pr(Y = 1 | \mathbf{A} = \mathbf{a}, \mathbf{X}, D = 0) Pr(\mathbf{A} = \mathbf{a} | \mathbf{X})]} \\
&= \frac{E[E[Y | S = 0, \mathbf{A} = \mathbf{a}, \mathbf{X}, D = 0] I(\mathbf{A} = \mathbf{a}) (1 - S)]}{E[E[Y | \mathbf{A} = \mathbf{a}, \mathbf{X}, D = 0] I(\mathbf{A} = \mathbf{a})]}
\end{aligned}$$

Estimated with:

$$\widehat{cFNR}(S, \mathbf{a}) = \frac{\sum_{i=1}^n \hat{\mu}_0(\mathbf{X}_i, \mathbf{A}_i, S = 0) (1 - S_i) I(\mathbf{A}_i = \mathbf{a})}{\sum_{i=1}^n \hat{\mu}_0^*(\mathbf{X}_i, \mathbf{A}_i) I(\mathbf{A}_i = \mathbf{a})}$$

11.2 Data generation for Section 4 simulations

Group	$P(Y^0 = 1)$	$P(D = 1 Y^0 = 1)$	$P(D = 1 Y^0 = 0)$
Minority: $A_1 = 1, A_2 = 1$	0.4	0.6	0.3
M1: $A_1 = 1, A_2 = 0$	0.4	0.6	0.3
M2: $A_1 = 0, A_2 = 1$	0.4	0.6	0.3
Majority: $A_1 = 0, A_2 = 0$	0.2	0.4	0.2

Table 1: Data generating parameters fixed in Section 4 simulations. We assume that treatment never increases probability of the event, i.e. $P(Y^1 = 1 | Y^0 = 0) = 0$. This simulation is based on an example in [29] demonstrating the differences between counterfactual and observational error rates for a single protected characteristic.

Table 1 shows data generating parameters that are fixed throughout the simulations in Section 4. Table 2 shows parameters manipulated in these simulations.

11.3 Data generation for Section 8 simulations

This section describes the simulation data generating process. To simplify notation, in this section we use \mathbf{A}^* to denote the vector of both protected characteristics and their

Group	Intervention strength	$P(A_1 = a_a, A_2 = a_2)$
Minority: $A_1 = 1, A_2 = 1$	A-C altered; D 0.8	A,C,D 0.06; B 0.04
M1: $A_1 = 1, A_2 = 0$	A-C 0.2; D altered	A,C,D 0.24; B 0.32
M2: $A_1 = 0, A_2 = 1$	A-C 0.2; D altered	A,C,D 0.14; B 0.32
Majority: $A_1 = 0, A_2 = 0$	A-D 0.2	A,C,D 0.56; B 0.32

Table 2: Data generating parameters manipulated in Section 4 simulations. Letters (**A - D**) refer to the four lettered panels of Figure 1. For parameters that are altered, the values used are depicted along the x-axis of each panel. Observational error rates are fixed at 0.1 (FPR) and 0.2 (FNR) for all groups in all plots.

interaction, e.g. $\mathbf{A}^* = (A_1, A_2, A_1A_2)$. We follow [29] in referring to $P(D = 1|Y^0 = 1, A_1, A_2)$ as the *opportunity rate* (shorted to “OR” in parameter names below) and $P(Y^0 = 1|A_1, A_2)$ as the *need rate*, (shortened to “NR”).

11.3.1 Protected characteristics, decision, and outcomes

$$P(A_1 = a_1, A_2 = a_2) = \text{Mult}(1, \boldsymbol{\pi}_{A_1, A_2})$$

$$\boldsymbol{\pi}_{A_1, A_2} = (\pi_{0,0}, \pi_{1,0}, \pi_{0,1}, \pi_{1,1})$$

$$= (0.58, 0.23, 0.13, 0.06)$$

$$\mathbf{X} \sim N((1, -1, 2, -2)^T, 0.3^2 * I_4)$$

$$Y^0 \sim \text{Ber}(\max\{\min\{p_{Y^0}, 0.995\}, 0.005\})$$

$$Y^1 \sim \text{Ber}(p_{Y^1})$$

$$D \sim \text{Ber}(\max\{\min\{\text{expit}[p_{OR}], 0.995\}, 0.005\})$$

$$Y = (1 - D)Y^0 + D * Y^1$$

11.3.2 Parameters for Y^0 and Y^1

$$p_{Y^0} = \text{expit}[\text{logit}(NR_{maj}) + (\mathbf{X}, \mathbf{A}^*) * (1, 1, 1, 1, \boldsymbol{\beta}_{A,Y^0})^T]$$

$$p_{Y^1} = \begin{cases} Y^0 = 0 & ; 0 \\ Y^0 = 1, A_1 = 1, A_2 = 1 & ; 1 - z_{min} \\ Y^0 = 1, A_1 = 1, A_2 = 0 & ; 1 - z_{M1} \\ Y^0 = 1, A_1 = 0, A_2 = 1 & ; 1 - z_{M2} \\ Y^0 = 1, A_1 = 0, A_2 = 0 & ; 0.8 \end{cases}$$

$$\boldsymbol{\beta}_{A,Y^0} = [\text{logit}(NR_M) - \text{logit}(NR_{maj}), \text{logit}(NR_M) - \text{logit}(NR_{maj}), \\ \text{logit}(NR_{maj}) - 2 * \text{logit}(NR_M) + \text{logit}(NR_{min})]$$

11.3.3 Parameters for D

$$\text{Trainingdata} : p_{OR} = \text{logit}(OR_{maj}) + (X_1, X_2, \mathbf{A}^*) * (1, 1, \boldsymbol{\beta}_{A,OR})^T$$

$$\text{Estimationdata} : p_{OR} = \text{logit}(OR_{maj}) + (X_1, X_2, \mathbf{A}^*, S) * (1, 1, \boldsymbol{\beta}_{A,OR}, \text{logit}(0.1))^T$$

$$\boldsymbol{\beta}_{A,OR} = [\text{logit}(OR_M) - \text{logit}(OR_{maj}), \text{logit}(OR_M) - \text{logit}(OR_{maj}), \\ \text{logit}(OR_{maj}) - 2 * \text{logit}(OR_M) + \text{logit}(OR_{min})]$$

11.3.4 Parameters controlling unfairness

- Scenario 1 (similar counterfactual error rates for all protected groups)

– Need rate:

$$* NR_{maj} = 0.6$$

$$* NR_M = 0.5$$

- * $NR_{min} = 0.4$
- Opportunity rate:
 - * $OR_{maj} = 0.2$
 - * $OR_M = 0.4$
 - * $OR_{min} = 0.6$
- Intervention strength:
 - * $z_{M1} = 0.2$
 - * $z_{M2} = 0.2$
 - * $z_{min} = 0.6$
- Predictors for random forest risk prediction model: \mathbf{X}
- Scenario 2 (Unfairness involving multiple groups)
 - Need rate and Opportunity rate: same as Scenario 1
 - Intervention strength:
 - * $z_{M1} = 0.3$
 - * $z_{M2} = 0.4$
 - * $z_{min} = 0.5$
 - Predictors for random forest risk prediction model: A_1, A_2, \mathbf{X}
- Scenario 3 (Unfairness involving one group)
 - Need rate:
 - * $NR_{maj} = 0.8$
 - * $NR_M = 0.4$

- * $NR_{min} = 0.4$

- Opportunity rate:

- * $OR_{maj} = 0.4$

- * $OR_M = 0.6$

- * $OR_{min} = 0.6$

- Intervention strength:

- * $z_{M1} = 0.2$

- * $z_{M2} = 0.2$

- * $z_{min} = 0.2$

- Predictors for random forest risk prediction model: A_1, A_2, \mathbf{X}